Research Article

Journal of Molecular Recognition

Received: 15 May 2012, Revised: 12 July 2012, Accepted: 13 July 2012, Published online in Wiley Online Library

(wileyonlinelibrary.com) DOI: 10.1002/jmr.2215

Kinetic and mechanistic differences in the interactions between caldendrin and calmodulin with AKAP79 suggest different roles in synaptic function

Christian Seeger[a,b], Xenia Gorny[c], Pasham Parameshwar Reddy[d], Constanze Seidenbecher[c] and U. Helena Danielson[a,b]*

The kinetic and mechanistic details of the interaction between caldendrin, calmodulin and the B-domain of AKAP79 were determined using a biosensor-based approach. Caldendrin was found to compete with calmodulin for binding at AKAP79, indicating overlapping binding sites. Although the AKAP79 affinities were similar for caldendrin (K_D = 20 nM) and calmodulin (K_D = 30 nM), their interaction characteristics were different. The calmodulin interaction was well described by a reversible one-step model, but was only detected in the presence of Ca^{2+}. Caldendrin interacted with a higher level of complexity, deduced to be an induced fit mechanism with a slow relaxation back to the initial encounter complex. It interacted with AKAP79 also in the absence of Ca^{2+}, but with different kinetic rate constants. The data are consistent with a similar initial Ca^{2+}-dependent binding step for the two proteins. For caldendrin, a second Ca^{2+}-independent rearrangement step follows, resulting in a stable complex. The study shows the importance of establishing the mechanism and kinetics of protein–protein interactions and that minor differences in the interaction of two homologous proteins can have major implications in their functional characteristics. These results are important for the further elucidation of the roles of caldendrin and calmodulin in synaptic function. Copyright © 2012 John Wiley & Sons, Ltd.

Keywords: postsynaptic density; A-kinase anchoring protein; caldendrin; calmodulin; surface plasmon resonance; induced fit

INTRODUCTION

Synapses are among the most complex organelles, harboring a large network of more than 1500 proteins (Klemmer *et al*., 2009) and with more than 1000 proteins in the postsynaptic proteome alone (Collins *et al*., 2006). These synaptic networks require a fine-tuned up and down regulation, occurring both at the genome and proteome levels. At the protein level, scaffolding or adaptor proteins play key roles in multiprotein signaling networks (Sanderson and Dell'Acqua, 2011). An important family of functionally related scaffold proteins are the A-kinase anchoring proteins (AKAPs). They coordinate signal transduction at different subcellular locations by anchoring protein kinase A, protein kinase C and the Ca^{2+}/calmodulin-dependent protein phosphatase calcineurin (Bhattacharyya *et al*., 2009; Dell'Acqua *et al*., 2006). The human orthologue AKAP79 appears to indirectly affect the synaptic plasticity of AMPA (α-amino-3 hydroxy-5-methyl-4-isooxazole-propionic acid) receptors via interactions with the postsynaptic density protein 95 and calcineurin (Bhattacharyya *et al*., 2009). Thereby, AKAP79 acts as an interface between glutamatergic signal transduction and intracellular signal transmission (Dell'Acqua *et al*., 2006). An additional AKAP79 interacting protein is calmodulin, a Ca^{2+}-regulated protein expressed ubiquitously (Chin and Means, 2000; Faux and Scott, 1997).

Here we have focused on caldendrin, a brain-specific Ca^{2+}-binding protein, with high sequence and structural similarity to calmodulin (Seidenbecher *et al*., 1998). It has a unique two-domain structure composed of a calmodulin-homologous terminus and an unrelated *N*-terminal part (Seidenbecher *et al*., 1998). The latter is thought to mediate the tight association of caldendrin with the subsynaptic cytoskeleton. Calmodulin and caldendrin have recently been found to bind to similar sequences of the B-domain of AKAP79 (Gorny *et al*., 2012). It appears that the B2-sequence (aa 75–97) is sufficient for calmodulin binding while caldendrin requires an extended binding site (aa 61–97).

The current study was undertaken in order to further investigate and compare the kinetic and mechanistic details of the interactions between calmodulin and caldendrin with the

* *Correspondence to: U. Helena Danielson, Department of Chemistry-BMC, Uppsala University, Box 576, SE-751 23 Uppsala, Sweden. E-mail: helena.danielson@kemi.uu.se*

a *C. Seeger, U. H. Danielson*
Beactica AB, Uppsala, Sweden

b *C. Seeger, U. H. Danielson*
Department of Chemistry-BMC, Uppsala University, Uppsala, Sweden

c *X. Gorny, C. Seidenbecher*
Neurochemistry/Molecular Biology, Leibniz Institute for Neurobiology, Magdeburg, Germany

d *P. P. Reddy*
PG Neuroplasticity, Leibniz Institute for Neurobiology, Magdeburg, Germany

Abbreviations: *AKAP, A-kinase anchoring protein; CDD, caldendrin; CAM, calmodulin; SPR, surface plasmon resonance; RU, resonance units.*

B-domain of AKAP79 and to determine whether the two proteins compete for binding to the overlapping binding sites. In addition, it was of interest to investigate if the interactions of calmodulin and caldendrin were equally influenced by calcium ions, because calmodulin is activated by intracellular calcium ion concentration at low micromolar concentrations (Berridge *et al*., 2000; Chin and Means, 2000).

For this study we used surface plasmon resonance (SPR) biosensor technology, a well-established method for kinetic and mechanistic analyses of molecular interactions. It has earlier been successfully employed for studying AKAP79 interacting proteins (Faux and Scott, 1997; Le *et al*., 2011) and has contributed to identifying and quantifying novel interactions of presynaptic scaffolding proteins (Wang *et al*., 2009). By a rigorous procedure involving a variety of experimental designs and data analysis procedures, it was possible to establish that the functional properties of caldendrin and calmodulin differ considerably, despite similarities in their interaction with AKAP79. The extended experimental procedure is motivated by the challenges in model discrimination and the requirement for extensive data when adopting complex interaction models. In addition, the lack of high quality experiments and comprehensive presentation of the underlying data often undermines the interpretations (Rich and Myszka, 2010, 2011). The present study is therefore unusually detailed, but enables an extended discussion on the relationship between interaction characteristics and protein function that provides a basis for further experiments using more physiologically relevant methods.

MATERIALS AND METHODS

Cloning, expression and purification of protein constructs

A detailed description of the cloning, expression and purification of the protein constructs employed is found elsewhere (Gorny *et al*., 2012). Briefly, the B-domain of AKAP79 (aa 61–116) was produced as a His-SUMO fusion protein (AKAP79-B-SUMO). Caldendrin was produced with glutathione *S*-transferase (GST) fused to the C-terminus (aa 137–298). GST alone was used as a negative control. The protein concentrations were determined by a colorimetric amido black assay (Popov *et al*., 1975). Calmodulin from human brain was purchased from GenWay Biotech. Inc. (San Diego, CA, USA).

SPR-based interaction studies

Surface plasmon resonance-based interaction studies were performed with Biacore T200, Biacore S51 and Biacore X100 instruments (GE Healthcare, Uppsala, Sweden). The instruments enabled slightly different experimental designs but did not differ in the quality of the generated data.

Sensor surface preparation

Standard amine coupling was used to immobilize AKAP79-B-SUMO to CM5 sensor chips (GE Healthcare). AKAP79-B-SUMO was injected at a concentration of 0.1 mg ml^{-1} in 10 mM Na-acetate (pH 5.5) for 5 min (5 µl min^{-1}). The running buffer during immobilization consisted of 10 mM Hepes, 150 mM Tris–HCl, 0.05% Tween-20, pH 7.4. An untreated flow cell was used as a reference surface.

Interaction analysis

Interaction analyses were performed in triplicates on freshly prepared sensor surfaces. Calmodulin was injected in twofold diluted concentration series from 250 to 8 nM using the multi-cycle kinetics mode of Biacore T200 and S51 instruments. Caldendrin–GST was analyzed using both multi-cycle (500–2 nM) and single-cycle kinetics mode (250–16 nM). The running buffer (buffer A) consisted of 25 mM Tris–HCl, 150 mM NaCl, 2 mM $CaCl_2$, 1 mM $MgCl_2$, 0.05% Tween-20, pH 7.4. Sensor surfaces were regenerated by injecting a short pulse (30 s) of a calcium-free buffer (buffer B, i.e., buffer A with $CaCl_2$ replaced by 50 µM EGTA).

Calcium-dependence experiments

Calcium-dependence experiments were performed at saturating Ca^{2+} conditions (2 mM, buffer A) and Ca^{2+}-free conditions (50 µM EGTA, buffer B). The calcium dependence of the calmodulin interaction with AKAP79 was analyzed using the "manual run" function of the Biacore X100 instrument by injecting 500 nM calmodulin over immobilized AKAP79-B-SUMO, both in the presence (buffer A) and absence (buffer B) of Ca^{2+}. Measurements with calmodulin and caldendrin–GST in the absence of Ca^{2+} (buffer B) were also performed by analyzing twofold diluted concentration series from 500 to 62 nM using the single-cycle kinetics mode of the Biacore X100 instrument.

Competition analysis

Competition analyses were performed in the presence of Ca^{2+} (buffer A). Calmodulin was injected at a concentration of 125 nM, both alone and in mixtures with caldendrin–GST (125, 250 and 500 nM). Sensorgrams of calmodulin (125 nM) and caldendrin–GST (125, 250 and 500 nM) were simulated using the BIAevaluation 4.1 software (GE Healthcare), and the experimental kinetic parameters were determined for each protein individually. Theoretical sensorgrams under non-competitive conditions were predicted as the sum of the simulated sensorgrams of caldendrin–GST and calmodulin alone. The responses at the end of the injections of both experimental and simulated sensorgrams were exported to Microsoft Excel (Microsoft Corporation, Redmond, WA, USA) for quantification and comparison of the signals.

Data analysis

Biacore T200 Evaluation Software 1.0 (GE Healthcare) was used for data analysis. Raw interaction data were double referenced by subtracting the data from a reference surface, followed by subtracting the average response of at least two blank samples. Determination of the interaction mechanisms was performed by global non-linear regression analysis using the following models:

- One-step interaction (Scheme 1)
- Two-step interaction (induced fit; Scheme 2)
- Heterogeneous ligand (Scheme 3)

$$A + B \underset{k_{-1}}{\overset{k_1}{\rightleftarrows}} AB$$

Scheme 1. Mechanism for a reversible one-step interaction between A and B, forming complex AB. The rate constants for the formation and dissociation of the complex are k_1 and k_{-1}, respectively.

Journal of Molecular Recognition

$$A + B \underset{k_{-1}}{\overset{k_1}{\rightleftarrows}} AB \underset{k_{-2}}{\overset{k_2}{\rightleftarrows}} ABx$$

Scheme 2. Mechanism for a reversible two-step interaction (induced fit) between A and B. An initial encounter complex AB is formed and subsequently transformed into ABx via a conformational change. The rate constants for the two steps are k_1 and k_{-1}, and k_2 and k_{-2}, respectively.

$$A + B1 \underset{k_{-1}}{\overset{k_1}{\rightleftarrows}} AB1 \qquad A + B2 \underset{k_{-2}}{\overset{k_2}{\rightleftarrows}} AB2$$

Scheme 3. Mechanism for the reversible one-step interaction (heterogeneous ligand) between A and B1, and A and B2. The two interactions occur independently in parallel. The rate constants for the two interactions are k_1 and k_{-1}, and k_2 and k_{-2}, respectively.

Analysis of mass transport limitation

The possibility that interactions were limited by mass transport was investigated by comparing the association rate constant (k_1) and the mass transfer coefficient (k_t) from each replicate essentially as described earlier (Karlsson, 1999). A qualitative analysis was also performed. It involved visual inspection of sensorgrams, primarily the part of the association phase just before steady-state is reached. Mass transport-limited sensorgrams are characterized by a linear association phase that abruptly reaches steady-state. Furthermore, fitted data were also inspected by using the *Check Kinetic Data* tool of the Biacore Evaluation Software that enables analysis of the effect of varying the magnitude of the rate constant on the sensorgram shape.

RESULTS

Design and validation of AKAP79 sensor surfaces for interaction analysis

A method for immobilization of AKAP79-B-SUMO to the carboxylated dextran matrix of CM5 sensor chips via amine coupling was devised, resulting in sensor surfaces with a surface density between 5000 and 8000 response units (RU) (Figure 1). These were stable over time, as indicated by an insignificant baseline drift of reference and blank subtracted data during interaction analysis

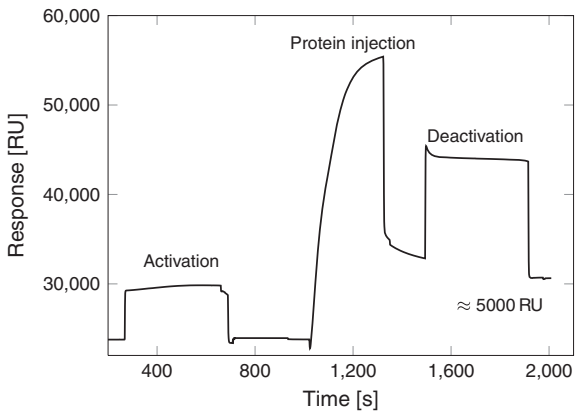

Figure 1. Immobilization of the B-domain of AKAP79 via amine coupling on CM5 sensor chips. Immobilization levels were approximately 5000 RU after deactivation of the sensor surface.

(≤0.5 RU/min). The functionality of the AKAP79 surfaces was validated by analysis of interactions with calmodulin, an acknowledged interaction partner for AKAP79.

The clear interaction between calmodulin and AKAP79 confirmed that the AKAP79 surface was functional (Figure 2A and B). As expected, no binding of calmodulin occurred in the absence of Ca^{2+} (Figure 2B and C). By injecting a series of calmodulin concentrations over the sensor surface with immobilized AKAP79 (Figure 2A), it was evident that the signals reached steady-state. Moreover, the maximal signal levels (R_{max}) indicated an apparent sensor surface functionality of ≈20%. The surface could be completely regenerated by injecting Ca^{2+}-free buffer (buffer B), confirming that the interaction was fully reversible. An alternative experimental design, involving varying injection times (Geitmann and Danielson, 2004), was also used to confirm that the interaction was effectively described by a reversible one-step model (Figure 3A). The simple interaction model was supported by experiments showing that the dissociation phase was not influenced by the length of the injection.

The one-step interaction model (Scheme 1; Figure 2A) was consequently used to estimate the association (k_1) and dissociation (k_{-1}) rate constants from three independent experiments ($n = 3$): $k_1 = 2 \times 10^6\ s^{-1}\ M^{-1}$ ($pk_1 = -6.3 \pm 0.4$) and $k_{-1} = 5 \times 10^{-2}\ s^{-1}$ ($pk_{-1} = 1.3 \pm 0.3$), corresponding to an affinity of $K_D = 30$ nM. (The standard deviations are provided for the negative logarithms of the values.) Although the interactions were relatively fast, they were not limited by mass transport as indicated by the mass transport coefficient k_t, which was approximately two orders of magnitude larger than the association constant k_a. Upon visual inspection, the calmodulin sensorgrams supported this interpretation because there was a smooth transition from the association phase to the steady-state phase. Furthermore, using the *Check Kinetic Data* tool to simulate sensorgrams, it could be demonstrated that the fitting was sensitive toward changes of the rate constants, a further indication that the interaction of calmodulin and AKAP79 was not limited by mass transport.

Interaction between AKAP79 and caldendrin

Caldendrin was also shown to interact with AKAP79, but with a higher level of complexity than observed with calmodulin (Figure 4A and B). The interaction was biphasic, with an initial rapid association followed by a slower phase that did not reach steady-state even after 7.5 min of injection (data not shown). Similarly, the dissociation was biphasic, with an initial rapid phase followed by a slow dissociation. In contrast to the efficient regeneration after the injections of calmodulin, it was not possible to regenerate the surface with Ca^{2+}-free buffer after injection of caldendrin. Experiments were therefore performed using the single-cycle kinetic mode in order to avoid artifacts due to incomplete regeneration of the surface (Figure 4A and B). Because caldendrin was studied as a GST-fusion protein, it was speculated that the interaction and its complexity could be a result of the fusion protein and not necessarily of the interaction of caldendrin itself. However, no interaction was detected when GST was injected under the same conditions as caldendrin (Figure 4A), excluding this explanation for the complexity of the interaction. Furthermore, the same results were obtained when reversing the experiment, that is, when immobilizing caldendrin-GST and using AKAP79-B-SUMO as analyte (Figure 5A). Qualitatively, the kinetics and normalized responses were comparable, a further indication of the negligible influence of GST on the interaction. The original setup, with immobilized

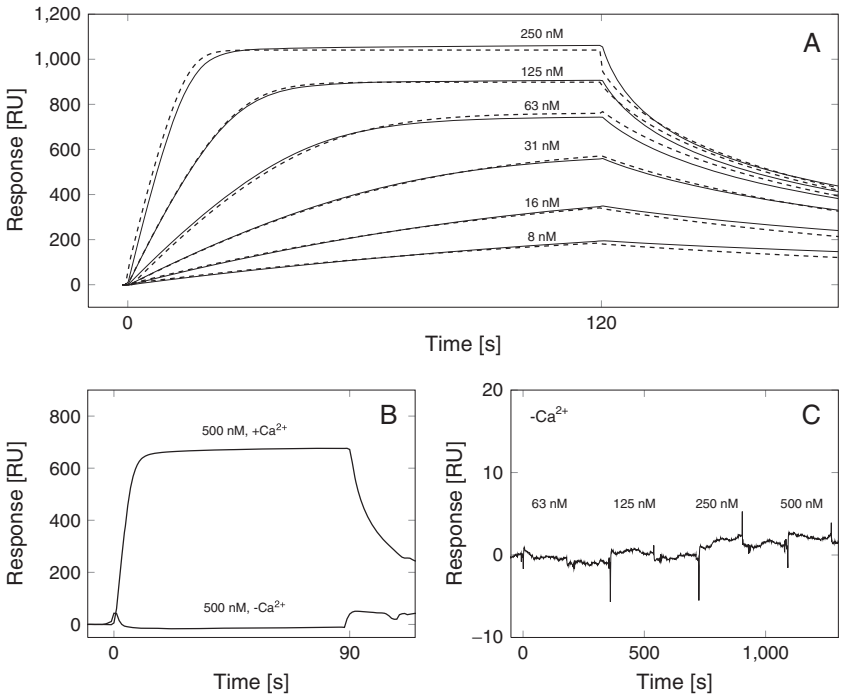

Figure 2. (A) Sensorgrams of calmodulin interacting with AKAP79. Calmodulin was injected in twofold dilution series from 250 to 8 nM over immobilized AKAP79-B-SUMO in the presence of Ca^{2+}. The dashed lines overlaying the double-referenced experimental data (solid) represent theoretical best fit lines obtained by global nonlinear regression analysis using a reversible one-step Langmuir interaction model (Scheme 1). (B) Calcium dependence of calmodulin interaction with AKAP79. Calmodulin (500 nM) was injected over immobilized AKAP79-B-SUMO in the presence (solid) and absence (dashed) of Ca^{2+}. The raw data were reference subtracted. (C) Calcium dependence of calmodulin interaction with AKAP79. Calmodulin (500–62 nM) was injected over immobilized AKAP79-B-SUMO using single-cycle kinetics in the absence of Ca^{2+}. The raw data were double referenced.

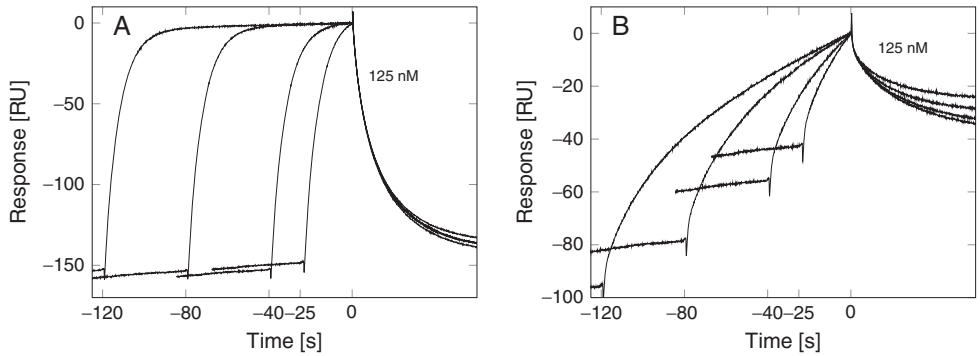

Figure 3. Effect of varying injection times (25, 40, 80 and 120 s) on dissociation kinetics of (A) calmodulin and (B) caldendrin–GST interacting with immobilized AKAP79-B-SUMO. Calmodulin and caldendrin–GST at a concentration of 125 nM were used in all injections. Reference subtracted raw data were aligned at the time for start of the dissociation.

AKAP79-B-SUMO (Figure 5B), was preferred because it provided higher data quality. When immobilizing caldendrin–GST, secondary effects were seen for high concentrations of AKAP79-B-SUMO that could not be rationally analyzed.

Determination of interaction mechanism and estimation of kinetic parameters

The interaction between caldendrin and AKAP79 was equally well described by a two-step model (Scheme 2) and a heterogeneous model (Scheme 3), as illustrated in Figure 6A. This is indicated both by similar fit qualities, expressed by the χ^2 parameter, and the high similarity of the curves fitted to the experimental data. It was also concluded that the components of the two binding events of a heterogeneous and a two-state model contribute similarly to the overall signal (Figure 6A).

As for calmodulin (Figure 3A), an alternative experimental design, where the injection times of caldendrin were varied, was used to establish the interaction mechanism (Figure 3B). The aim was to determine whether the dissociation phase varied considerably with the injection time. Because the sensorgrams of caldendrin did not reach steady-state, it was not useful to simply align the sensorgrams with respect to the time for dissociation start (Figure 3B), as was useful for calmodulin (Figure 3A). A more elaborate experimental design was therefore used where caldendrin was

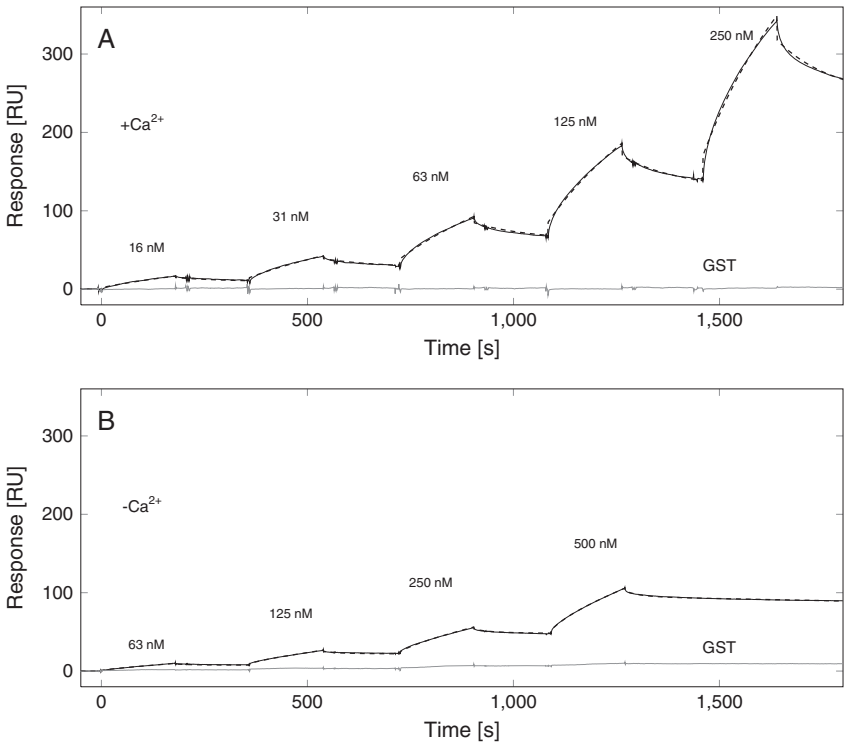

Figure 4. Sensorgrams of caldendrin interacting with AKAP79 in the (A) presence and (B) absence of 2 mM Ca^{2+}. Caldendrin was injected as caldendrin–GST in twofold dilution series (solid) over immobilized AKAP79-B-SUMO using single-cycle kinetics. The dashed lines overlaying the double-referenced sensorgrams of caldendrin-GST represent theoretical best fit lines obtained by global nonlinear regression analysis using a two-step model (Scheme 2). GST (solid, gray) served as a negative control and was injected under the same conditions as caldendrin–GST.

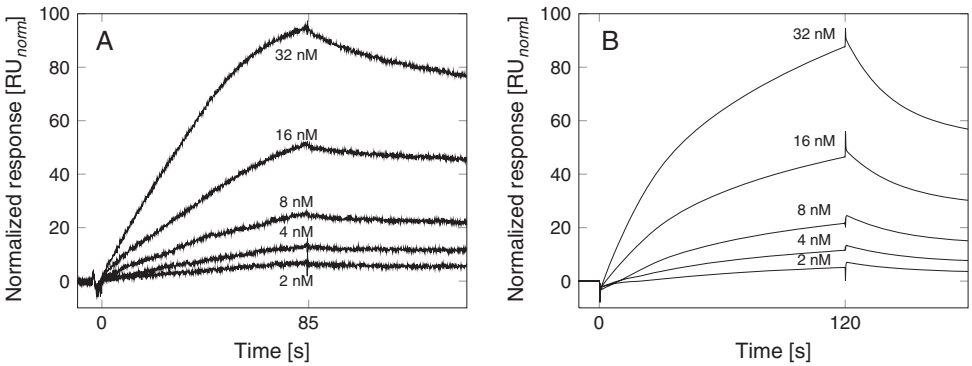

Figure 5. Sensorgrams of caldendrin interacting with AKAP79 in the presence of Ca^{2+}. (A) AKAP79 was injected as AKAP79-B-SUMO over immobilized caldendrin–GST in two-fold dilution series (32–2 nM) using multi-cycle kinetics mode. The raw data were double referenced and normalized with respect to the different molecular weights of the immobilized protein and analyte: $RU_{norm} = RU \times M_{caldendrin-GST}/M_{AKAP79\text{-}B\text{-}SUMO}$. (B) Caldendrin was injected as caldendrin–GST in twofold dilution series (31–2 nM) over immobilized AKAP79-B-SUMO using multi-cycle kinetics mode. Double-referenced raw data were normalized as $RU_{norm} = RU \times M_{AKAP79\text{-}B\text{-}SUMO}/M_{caldendrin\text{-}GST}$.

analyzed at different concentrations and injection times (Figure 7) (Geitmann *et al.*, 2011). It was assumed that global non-linear regression analysis of the data set with different concentrations and injection times would clearly show that one of the models cannot sufficiently describe the interaction. However, this was not the case as the data could be described equally well with a two-step and a heterogeneous binding model (Figure 7). The experimental data did therefore not provide conclusive evidence for a certain model even with this extended experimental design. Nevertheless, there is logical support for a two-step model (see Section on Discussion). With this model, the kinetic parameters of the interaction were determined as follows: $k_1 = 9 \times 10^3\ s^{-1}\ M^{-1}$ ($pk_1 = -3.9 \pm 0.4$, $n = 3$), $k_{-1} = 4 \times 10^{-3}\ s^{-1}$ ($pk_{-1} = 2.4 \pm 0.1$), $k_2 = 3 \times 10^{-3}\ s^{-1}$ ($pk_2 = 2.5 \pm 0.1$), $k_{-2} = 2 \times 10^{-4}\ s^{-1}$ ($pk_{-2} = 3.8 \pm 0.1$), corresponding to an affinity of $K_D = 20$ nM. The apparent sensor surface functionality was ≈20%, which is similar to that obtained with calmodulin, confirming that the analyses of the two proteins are comparable.

Calcium dependence of caldendrin binding

The Ca^{2+} dependence of the interaction between caldendrin and AKAP79 was also studied (Figure 6B). In contrast to calmodulin (Figure 2B and C), caldendrin was found to interact weakly with AKAP79 under Ca^{2+}-free conditions (50 μM EGTA instead of

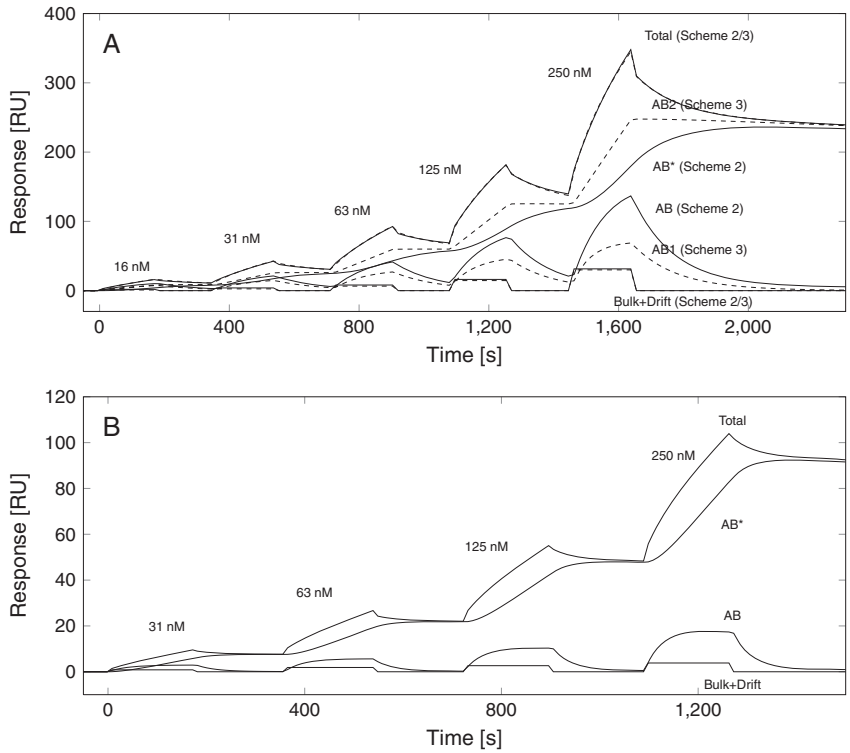

Figure 6. (A) The relative contribution of the components of (a) a 2-step model (AB, AB* from Scheme 2, solid), and (b) a heterogeneous model (AB1, AB2 from Scheme 3, dashed) describing the interaction between caldendrin and AKAP79. The models were fitted to double-referenced single-cycle kinetic data of caldendrin–GST interacting with AKAP79-B-SUMO in the presence of Ca^{2+}. (B) The relative contribution of the components of a two-step model (AB, AB* from Scheme 2) describing the interaction between caldendrin and AKAP79 in the absence of Ca^{2+}. The raw data were double referenced.

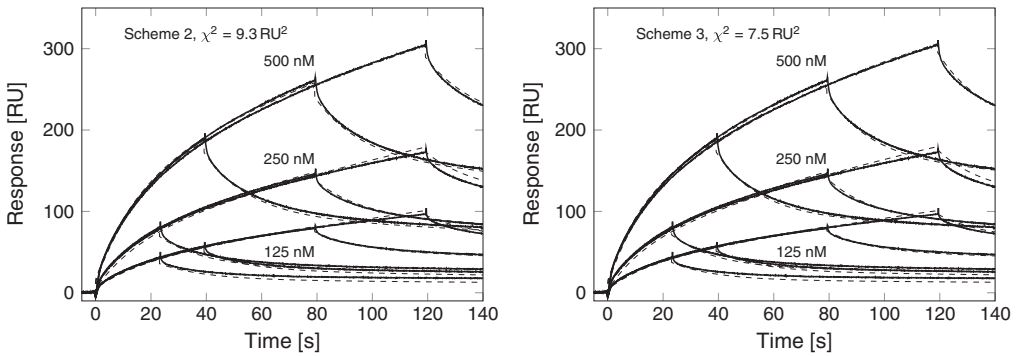

Figure 7. Comparison of two interaction models globally fitted to binding data of caldendrin and AKAP79. Caldendrin was injected as caldendrin–GST with different injection times (25, 40, 80 and 120 s) and different concentrations (125, 250 and 500 nM) over immobilized AKAP79-B-SUMO. A two-step model (Scheme 2, dashed, left) and a heterogeneous binding model (Scheme 3, dashed, right) were fitted to the reference subtracted data (solid).

2 mM Ca^{2+}). Although the kinetic profile of the caldendrin interactions with AKAP79 was similar in the absence and presence of calcium, the binding levels were up to 10-fold lower under Ca^{2+}-free conditions (Figure 6B). The kinetic parameters indicated that calcium primarily influenced the first step, which has both slower association ($k_{1-\text{calcium}} \approx 0.4 \cdot k_{1+\text{calcium}}$) and faster dissociation ($k_{-1-\text{calcium}}$ $5 \times k_{-1+\text{calcium}}$) in the absence of calcium. Furthermore, the contribution of the two components of the mechanistic model to the overall signal is influenced considerably by the presence of high Ca^{2+} concentrations (2 mM). In the presence of Ca^{2+}, both components of the interaction contribute similarly to the overall signal (Scheme 2; Figure 6A), whereas in the absence of Ca^{2+}, the contribution of the first component (AB, Scheme 2) is considerably reduced compared with the second component (AB*, Scheme 2) as shown in Figure 6B.

Competition between calmodulin and caldendrin

Competition between calmodulin and caldendrin for binding to AKAP79 was explored in the presence of 2 mM Ca^{2+} by injecting 125 nM calmodulin alone and in mixtures with caldendrin–GST (125, 250 and 500 nM). The theoretical sensorgrams for a non-competitive interaction were simulated as the sum of the signals of calmodulin and caldendrin–GST, on the basis of the kinetic parameters determined for the individual interactions. The total signal was normalized with respect to the molecular weight of

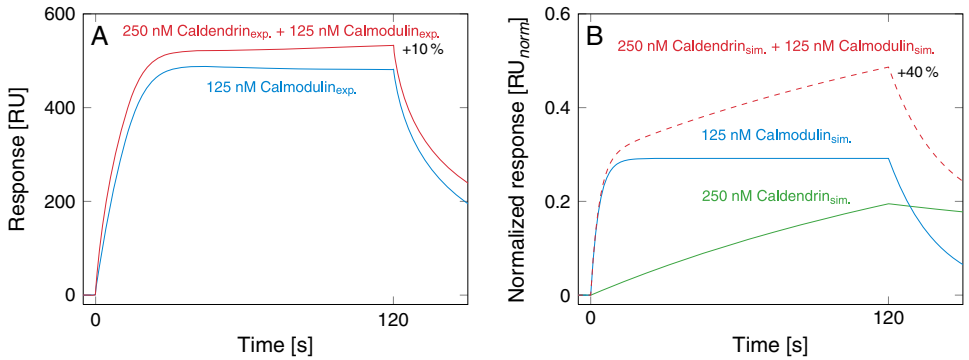

Figure 8. Competition analysis between calmodulin and caldendrin. (A) Calmodulin was injected at a concentration of 125 nM alone (blue) and together with 250 nM caldendrin–GST (red) in the presence of 2 mM Ca^{2+}. Raw data were reference subtracted. The relative increase in signal level (+10%) at the end of the injection is indicated. (B) Simulated data of the interactions of 125 nM calmodulin (blue), 250 nM caldendrin–GST (green) and the theoretical signal under non-competitive conditions (red, dashed). The reference-subtracted data were normalized with respect to the molecular weight of the analyte (caldendrin–GST 45.5 kDa, $R_{max} \equiv 1.00$, calmodulin 16 kDa $R_{max} \equiv 0.35$).

the injected proteins (caldendrin–GST 45.5 kDa, $R_{max} \equiv 1.00$, calmodulin 16 kDa $R_{max} \equiv 0.35$). Figure 8 shows the experimental (Figure 8A) and simulated (Figure 8B) data of the competition analysis at 125 nM calmodulin and 250 nM caldendrin–GST. The results show that the experimental relative increase of the response levels at the end of the injections was less than 50% of the predicted relative increase of the simulation, strongly indicating competition of calmodulin and caldendrin–GST. Competition was assessed for caldendrin–GST concentrations of 125, 250 and 500 nM. As a negative control, sensorgrams for a calmodulin and caldendrin–GST concentration of 31 nM were also simulated. The assumption was that calmodulin and caldendrin–GST, when injected close to its K_D value will occupy approximately 50% of the binding sites and not compete with each other. The experimental relative increase of the mixture is close to the predicted increase from the simulation, therefore supporting the hypothesis that no competition occurs when calmodulin and caldendrin–GST are injected at a concentration around their K_D values. Furthermore, competition was not predicted at a caldendrin–GST concentration of 500 nM, a concentration approximately 25 times above the K_D value, supported by the experimental data.

DISCUSSION

A new assay and its features

The new biosensor assay for analysis of interactions with AKAP79, a key scaffolding protein in the postsynaptic density (Sanderson and Dell'Acqua, 2011), proved to be useful for characterizing its interactions with calmodulin and caldendrin. The immobilized protein was stable over time and had an apparent functionality typical for biosensor surfaces and more than adequate for the current experiments. A series of experimental designs were exploited in order to establish the mechanism and the kinetic parameters of the interactions and to elucidate the functional differences between the interactions for caldendrin and calmodulin. Because the sensor surfaces could not be sufficiently regenerated after caldendrin injections, experiments were performed using both conventional multi-cycle analysis and single-cycle injections. The latter mode is especially useful for analytes that dissociate poorly or not at all from a sensor surface (Glück *et al.*, 2011; Karlsson *et al.*, 2006). Furthermore, experiments with different injection times and buffer conditions, as well as with simultaneous injections of the two analytes at different molar ratios, proved very informative.

The mechanism of calmodulin and caldendrin interactions with AKAP79

Both calmodulin and caldendrin–GST clearly interacted with AKAP79, but differed in their mechanism and Ca^{2+} dependence. Calmodulin interacted according to a reversible one-step model (Scheme 1) in the presence of Ca^{2+}, whereas no interaction was detected in its absence. In contrast, the biosensor analyses revealed that the interaction between caldendrin and AKAP79 was more complex and not adequately described by a simple one-step model. Caldendrin data were therefore analyzed with respect to a selection of alternative interaction models. The analysis presented in the results section includes two models (Schemes 2 and 3) that effectively described the data. The heterogeneous model (Scheme 3) represents two possible scenarios. The first assumes two independent binding sites, each interacting with the ligand in a 1:1 stoichiometry but with different kinetics. The second scenario assumes only a single binding site on the protein, but that the protein is present in two different forms with different interaction characteristics for the ligand, reflecting protein structure heterogeneity rather than multiple binding sites.

The two-step model (induced fit) also described the caldendrin data well. It represents an interaction where caldendrin forms an initial encounter complex with AKAP79 that rearranges to form a second stable complex. The model can involve an initial binding between caldendrin and a primary subsite, followed by a second binding to a secondary subsite, or simply a structural rearrangement of a single complete binding site. A number of different features of caldendrin suggest that this is the most plausible model, although it is not possible to exclude the heterogeneous model at this stage.

For example, both caldendrin and calmodulin contain an α-helical region that separates both helix-loop-helix motifs (EF hands). In caldendrin, it is four amino acids longer than calmodulin (Laube *et al.*, 2002; Seidenbecher *et al.*, 1998), adding to the structural flexibility that may provide the dynamic foundation for an induced fit mechanism. Further support for such a mechanism comes from recent structural and calorimetric studies (Findeisen and Minor, 2010). It was demonstrated that a caldendrin variant acts both via a C-lobe and N-lobe at the voltage-gated calcium

channel 1.2, each lobe having different functions. Interestingly, it was proposed that the protein needs to undergo a conformational change to allow both lobes to bind, which is in agreement with an induced fit mechanism. Whether the same structural rearrangements occur during the interaction between caldendrin and AKP79 remains unknown but would be supported by the present kinetic data.

Because the direct binding experiments and global regression analysis of the data did not give conclusive data for the identification of the interaction mechanism for caldendrin with AKAP79, a variety of additional experiments were performed. Taken together, and despite the adequacy of the heterogeneous model for regression analysis of the caldendrin data, there is weak experimental support for a heterogeneous mechanism. Instead, the data are consistent with a two-step model with a slow dissociation from the complex formed in the second step, as will be outlined subsequently.

There was initially a concern with the use of caldendrin in the form of a GST fusion construct although it has earlier been used for SPR-based interaction analysis with recoverin (Fries *et al.*, 2010). Alternative constructs (immobilized AKAP79-B-GST instead of AKAP79-B-SUMO and caldendrin-SUMO as analyte instead of caldendrin-GST) were therefore also tested but did not give useful data (not shown). Because GST alone did not interact with AKAP79, it was concluded that the construct was a valid model system for these experiments. It was also speculated that the observed heterogeneity of the caldendrin interaction was due to dimerization of caldendrin, either via caldendrin itself (Fries *et al.*, 2010) or induced by GST. By reversing the assay and immobilizing caldendrin–GST on the sensor surface, it was assumed that dimerization of caldendrin–GST during the interaction analysis should be prevented and that the sensorgrams should clearly differ. When injecting AKAP79-B-SUMO, the complex kinetics were qualitatively maintained (Figure 5A), suggesting that dimerization of caldendrin–GST, potentially via GST, was not the cause for the complex kinetic mechanism. An interaction model, taking into account that caldendrin interacts with AKAP79-B-SUMO both as a monomer and a dimer, was fitted to the data as well but did not effectively describe the data (data not shown) and was rejected. Furthermore, it is not known whether caldendrin can bind to AKAP79 as a dimer and at what ratio caldendrin is present as a monomer and dimer, making the use of a model assuming this possibility not applicable with the present information.

Pull-down experiments using different AKAP79-B-domain constructs have localized the calmodulin binding site to a central sequence of the B-domain (aa 75–97; Gorny *et al.*, 2012). The current data suggest that this is a single site to which calmodulin interacts in a reversible manner, however restricted to the presence of Ca^{2+} (Scheme 4).

The determined affinity of calmodulin ($K_D = 30$ nM) with the B-domain is practically the same as that previously determined for full-length AKAP79 (Faux and Scott, 1997) and reported to be within a physiological range. Despite similar affinity, both the association and dissociation constants determined by Faux and Scott ($k_1 = 2 \times 10^5\ s^{-1}\ M^{-1}$ and $k_{-1} = 5 \times 10^{-3}\ s^{-1}$) are one order of magnitude lower than the determined in the present study ($k_1 = 2 \times 10^6\ s^{-1}\ M^{-1}$ and $k_{-1} = 5 \times 10^{-2}\ s^{-1}$). This might be attributed to different assay conditions and/or the different instruments employed. Closed systems, such as the IAsys biosensor system used by Faux and Scott, tend to underestimate association constants and overestimate dissociation constants, especially with high-affinity interactions due to ligand depletion and rebinding (Edwards *et al.*, 1998).

$$CaM + AKAP \underset{k_{-1}}{\overset{k_1}{\rightleftarrows}} CaM - AKAP$$

Scheme 4. Reversible one-step interaction between calmodulin and AKAP, consistent with the current data. The interaction is calcium dependent and CaM-AKAP is not detected in the absence of calcium.

The experiments in the preceding study (Gorny *et al.*, 2012) showed that caldendrin binds to the same sequence as calmodulin, but that additional amino acids located *N*-terminally to the calmodulin binding site are required (aa 61–76) for binding. It is therefore not surprising that caldendrin and calmodulin appeared to compete in pull-down experiments in the presence of Ca^{2+} (Gorny *et al.*, 2012). The SPR-based experiments confirmed the competition between calmodulin and caldendrin–GST with calmodulin effectively blocking the caldendrin–GST binding. In this particular analysis, it was helpful to use simulated data to support the experimental data when assessing competition.

The calmodulin–AKAP79 interaction required calcium for detectable binding, although caldendrin interacted weakly with AKAP79 in the absence but more efficiently at high (2 mM) calcium concentrations, also supported by pull-down experiments (Gorny *et al.*, 2012). The difference in calcium dependence for caldendrin and calmodulin binding to AKAP79 is consistent with a mechanism where the first step requires calcium for detectable binding (Schemes 4 and 5), being the same for both proteins. But the calcium effect observed for caldendrin actually arises from the second step, although it appears to be calcium independent. This conundrum is explained by the fact that caldendrin can interact with AKAP79 even in the absence of calcium, but more inefficiently. Still, this is enough for some of the initial encounter complex to be transformed into the second stable complex (Scheme 5). This will trap some caldendrin whereby a stable caldendrin–AKAP79 complex will build up over time. This does not occur for calmodulin, which therefore cannot be detected to interact in the absence of calcium.

Kinetic characteristics and functional consequences

The competition data of caldendrin and calmodulin show that calmodulin is more efficient in binding to AKAP79 than caldendrin. This is consistent with the difference in kinetics of the AKAP79 interaction for the two proteins. The initial step is more efficient for calmodulin ($k_1 = 2 \times 10^6\ s^{-1}\ M^{-1}$), having an approximately 200 times faster association rate than caldendrin ($k_1 = 9 \times 10^3\ s^{-1}\ M^{-1}$). As calmodulin is highly regulated by calcium (Berridge *et al.*, 2000; Chin and Means, 2000), fast kinetics are advantageous to mediate its transient effects. In contrast, the ability of caldendrin to rearrange and form a second stable complex will result in a long-lasting effect. Assuming that the kinetics are the same *in vivo* as in the system used in these experiments, it would take approximately 10 h until caldendrin is fully dissociated from AKAP79. Furthermore, the interaction cannot simply be reversed by removal of calcium, as for calmodulin. Despite the similar overall affinities of the two interactions, the two proteins can thus be expected to result in very different effects *in vivo*.

$$CDD + AKAP \underset{k_{-1}}{\overset{k_1}{\rightleftarrows}} CDD - AKAP \underset{k_{-2}}{\overset{k_2}{\rightleftarrows}} \text{“}CDD - AKAP\text{“}$$

Scheme 5. Hypothesized induced fit interaction between caldendrin and AKAP, consistent with the current data and supported by other experimental data. The first step is calcium dependent, but not the second. Due to the high stability of “CDD-AKAP”, complex formation is detected even in the absence of calcium.

The use of biosensor technology for elucidation of function, via detailed kinetic and mechanistic studies of protein–protein is not common. Instead, it is sometimes simply recognized as one of many methods for identifying and confirming novel interactions (Berggard *et al*., 2007; Dwane and Kiely, 2011), as we and others have also performed for other scaffolding proteins (Fukunaga *et al*., 2005; Larsson *et al*., 2003; Wang *et al*., 2009) and in the initial study of caldendrin interactions with AKAP79 (Gorny *et al*., 2012). The quantification is often limited to determination of affinities, assuming simple interaction models even when the interaction mechanism is clearly more complex (Fukunaga *et al*., 2005). The discrimination of different models is often challenging, requiring high quality data, extensive experimental work and rigorous data analysis. However, when using the technique to its full potential, it is possible to obtain detailed kinetic and mechanistic information that can be used for the increased understanding of function, as a complement to physiological studies.

CONCLUSIONS

The present study confirms that caldendrin and calmodulin interact with the B-domain of AKAP79 at overlapping binding sites but exhibit different interaction characteristics. The two-step interaction mechanism for caldendrin results in a unique ability to form a stable complex, even in the absence of calcium. This difference between caldendrin and calmodulin is expected to considerably influence their functional properties and regulation *in vivo*. For example, the potential physiological relevance of the difference in calcium dependence of the two proteins as it can be interpreted such that Ca^{2+} has a transient reversible regulatory effect on the interaction between calmodulin and AKAP79, consistent with typical calmodulin function. Caldendrin instead may have an interaction with AKAP79 that is not strictly dependent on calcium, although more efficient in its presence. It is possible that there are additional interactions *in vivo*, with other regions of AKAP79 or other proteins, that modulate the ones studied here, for example resulting in an efficient dissociation of caldendrin from AKAP79. It is therefore premature to use these data for interpretation of the physiological mechanisms and functions of these interactions, but the current findings provide a framework for elucidating the role of these interactions by future experiments.

Acknowledgements

The research leading to these results has received funding from the European Union Seventh Framework Programme under grant agreement FP7-People-ITN-2008-238055 ("BrainTrain" project), the DFG (SFB779, TPA08 and TP B08; Kr1897/3-1), the Leibniz Graduate School LGS, and the Swedish Research Council (VR). The authors thank Karl Andersson and Malin Elinder for discussion and critical reading of the manuscript. The authors have no conflict of interest to declare.

REFERENCES

Berggard T, Linse S, James P. 2007. Methods for the detection and analysis of protein-protein interactions. *Proteomics* **7**: 2833–2842.

Berridge MJ, Lipp P, Bootman MD. 2000. The versatility and universality of calcium signalling. *Nat. Rev. Mol. Cell Biol.* **1**: 11–21.

Bhattacharyya S, Biou V, Xu W, Schlüter O, Malenka RC. 2009. A critical role for PSD-95/AKAP interactions in endocytosis of synaptic AMPA receptors. *Nat. Neurosci.* **12**: 172–181.

Chin D, Means AR. 2000. Calmodulin: a prototypical calcium sensor. *Trends Cell Biol.* **10**: 322–328.

Collins MO, Husi H, Yu L, Brandon JM, Anderson CNG, Blackstock WP, Choudhary JS, Grant SGN. 2006. Molecular characterization and comparison of the components and multiprotein complexes in the postsynaptic proteome. *J. Neurochem.* **97**: 16–23.

Dell'Acqua ML, Smith KE, Gorski JA, Horne EA, Gibson ES, Gomez LL. 2006. Regulation of neuronal PKA signaling through AKAP targeting dynamics. *Eur. J. Cell Biol.* **85**: 627–633.

Dwane S, Kiely PA. 2011. Tools used to study how protein complexes are assembled in signaling cascades. *Bioeng. Bugs* **2**: 247–259.

Edwards PR, Maule CH, Leatherbarrow RJ, Winzor DJ. 1998. Second-order kinetic analysis of IAsys biosensor data: its use and applicability. *Anal. Biochem.* **263**: 1–12.

Faux MC, Scott JD. 1997. Regulation of the AKAP79-protein kinase C interaction by Ca^{2+}/calmodulin. *J. Biol. Chem.* **272**: 17038–17044.

Findeisen F, Minor DL. 2010. Structural basis for the differential effects of CaBP1 and calmodulin on Ca(V)1.2 calcium-dependent inactivation. *Structure* **18**: 1617–1631.

Fries R, Reddy PP, Mikhaylova M, Haverkamp S, Wei T, Muller M, Kreutz MR, Koch KW. 2010. Dynamic cellular translocation of caldendrin is facilitated by the Ca^{2+}–myristoyl switch of recoverin. *J. Neurochem.* **113**: 1150–1162.

Fukunaga Y, Matsubara M, Nagai R, Miyazawa A. 2005. The interaction between PSD-95 and Ca^{2+}/calmodulin is enhanced by PDZ-binding proteins. *J. Biochem.* **138**: 177–182.

Geitmann M, Dahl G, Danielson UH. 2011. Mechanistic and kinetic characterization of hepatitis C virus NS3 protein interactions with NS4A and protease inhibitors. *J. Mol. Recognit.* **24**: 60–70.

Geitmann M, Danielson UH. 2004. Studies of substrate-induced conformational changes in human cytomegalovirus protease using optical biosensor technology. *Anal. Biochem.* **332**: 203–214.

Glück JM, Koenig BW, Willbold D. 2011. Nanodiscs allow the use of integral membrane proteins as analytes in surface plasmon resonance studies. *Anal. Biochem.* **408**: 46–52.

Gorny X, Mikhaylova M, Seeger C, Reddy PP, Reissner C, Schott BH, Danielson UH, Kreutz MR, Seidenbecher C. 2012. AKAP79/150 interacts with the neuronal calcium-binding protein caldendrin. *J. Neurochem.* **1**: 714–726.

Karlsson R. 1999. Affinity analysis of non-steady-state data obtained under mass transport limited conditions using BIAcore technology. *J. Mol. Recognit.* **12**: 285–292.

Karlsson R, Katsamba PS, Nordin H, Pol E, Myszka DG. 2006. Analyzing a kinetic titration series using affinity biosensors. *Anal. Biochem.* **349**: 136–147.

Klemmer P, Smit A, Li K. 2009. Proteomics analysis of immuno-precipitated synaptic protein complexes. *J. Proteomics* **72**: 82–90.

Larsson M, Hjalm G, Sakwe AM, Engstrom A, Hoglund AS, Larsson E, Robinson RC, Sundberg C, Rask L. 2003. Selective interaction of megalin with postsynaptic density-95 (PSD-95)-like membrane-associated guanylate kinase (MAGUK) proteins. *Biochem. J.* **373**: 381–391.

Laube G, Seidenbecher C, Richter K, Dieterich D, Hoffmann B, Landwehr M, Smalla K, Winter C, Böckers T, Wolf G. 2002. The neuron-specific Ca^{2+}-binding protein caldendrin: gene structure, splice isoforms, and expression in the rat central nervous system. *Mol. Cell Neurocsci.* **19**: 459–475.

Le AV, Tavalin SJ, Dodge-Kafka KL. 2011. Identification of AKAP79 as a protein phosphatase 1 catalytic binding protein. *Biochemistry* **50**: 5279–5291.

Popov N, Schmitt M, Schulzeck S, Matthies H. 1975. Reliable micromethod for determination of the protein content in tissue homogenates. *Acta Biol. Med. Ger.* **34**: 1441–1446.

Rich RL, Myszka DG. 2010. Grading the commercial optical biosensor literature class of 2008: the mighty binders. *J. Mol. Recognit.* **23**: 1–64.

Rich RL, Myszka DG. 2011. Survey of the 2009 commercial optical biosensor literature. *J. Mol. Recognit.* **24**: 892–914.

Sanderson JL, Dell'Acqua ML. 2011. AKAP signaling complexes in regulation of excitatory synaptic plasticity. *Neuroscientist* **17**: 321–336.

Seidenbecher CI, Langnaese K, Sanmartı-Vila L, Boeckers TM, Smalla KH, Sabel BA, Garner CC, Gundelfinger ED, Kreutz MR. 1998. Caldendrin, a novel neuronal calcium-binding protein confined to the somatodendritic compartment. *J. Biol. Chem.* **273**: 21324–21331.

Wang X, Hu B, Zieba A, Neumann NG, Kasper-Sonnenberg M, Honsbein A, Hultqvist G, Conze T, Witt W, Limbach C, Geitmann M, Danielson H, Kolarow R, Niemann G, Lessmann V, Kilimann MW. 2009. A protein interaction node at the neurotransmitter release site: domains of Aczonin/Piccolo, Bassoon, CAST, and rim converge on the N-terminal domain of Munc13-1. *J. Neurosci.* **29**: 12584–12596.

